

# Formation of Hydrogen-Bonded Structures in Jet-Cooled Complexes of a Chiral Chromophore Studied by IR/UV Double Resonance Spectroscopy: Diastereoisomeric Complexes of ( $\pm$ )-2-Naphthyl-1-ethanol with ( $\pm$ )-2-Amino-1-propanol

K. Le Barbu, F. Lahmani, and A. Zehnacker-Rentien\*

Laboratoire de Photophysique Moléculaire, CNRS UPR3361, Bâtiment 210, Université de Paris XI, 91405 Orsay Cédex, France

Received: December 31, 2001; In Final Form: March 7, 2002

The structure of weakly bound diastereoisomeric complexes of ( $\pm$ )-2-naphthyl-1-ethanol with ( $\pm$ )-2-amino-1-propanol (alaninol) has been interrogated by means of laser-induced fluorescence and IR fluorescence dip spectroscopy. The diastereoisomers have been discriminated on the basis of the complexation-induced shift of the  $S_0$ – $S_1$  transition of the chromophore. The heterochiral complex exists under one dominant fluorescent form, while two isomers have been detected for the homochiral complex, with a dramatically different spectroscopic signature in the  $\nu(\text{OH})$  region. The solely observed heterochiral complex involves an  $\text{OH}\cdots\text{O}$  bond from the chromophore to alaninol, with a quasi retention of the most stable structure of the amino alcohol molecule (intramolecular hydrogen bond). One of the homochiral isomers adopts the same  $\text{OH}\cdots\text{O}$  structure while the second homochiral one involves a  $\text{OH}\cdots\text{N}$  bond to alaninol, whose conformation differs from that of the most stable isolated fragment (absence of the intramolecular hydrogen bond). The observation of both structures of the homochiral complex leaves no doubt as to the fact that isomers containing energetically disfavored fragments can be formed in the supersonic expansion. Moreover, the  $\text{OH}\cdots\text{N}$  structure is only observed in the homochiral complex, which seems to indicate that the two enantiomers of the chromophore do not select the same conformation of alaninol during the complexation process.

## Introduction

Chiral recognition lies at the very foundation of chemical processes related to life chemistry and is thought to take place through the formation of contact pairs involving specific interactions. Owing to the transient nature of the complexes at play, a molecular-scale approach to the nature of the interactions responsible for chiral discrimination is difficult to achieve in the condensed phase. The study of jet-cooled complexes overcomes the transient character of the diastereoisomeric adducts and the interference from the medium.<sup>1</sup> We have pioneered the study of chiral discrimination in jet-cooled complexes<sup>2</sup> and have shown that it is possible to discriminate between the enantiomers of a chiral molecule by complexation with a chiral fluorescent chromophore acting as a selector:<sup>3,4</sup> the homo- and heterochiral pairs are characterized by the nonequivalence of their structure and therefore possess a different interaction energy both in the ground state and the excited state, which results in a different shift of the  $S_0$ – $S_1$  transition relative to the bare chromophore. Since then, REMPI and laser induced fluorescence measurements have been applied to study weakly bound complexes of chiral molecules: further work in our group and others includes measurements of the relative stability of the diastereoisomeric complexes<sup>5,6</sup> and the study of the enantioselectivity of the excited-state deactivation processes.<sup>7</sup> As the molecules under study are quite flexible and can coexist under different conformers in the conditions of the supersonic expansion, conformer specific spectroscopic methods are required: UV/UV depletion (hole-burning) spectroscopy<sup>8,9</sup> has been applied to provide evidence on the role of conforma-

tional isomerism in chiral discrimination. However, the experiments mentioned above rest on the difference between the excited (or ionic) state properties and those of the ground state: no molecular structure of the complex can be directly inferred from the experimental results. This has therefore motivated microwave or infrared spectroscopy studies which give direct information on the ground-state structure.

Discrimination between the homochiral and the heterochiral dimers of glycidol has been recently obtained by Fourier transformed infrared spectroscopy.<sup>10</sup> A microwave study of the heterochiral dimer of butan-2-ol has also been recently reported.<sup>11</sup> The technique of IR fluorescence or ion dip spectroscopy provides a well-adapted tool to probe the ground-state OH stretch frequencies in isolated H-bonded molecules and complexes and to characterize the binding sites in such systems. It has been applied to phenol<sup>12</sup> and benzene complexes,<sup>13–16</sup> to bridged complexes of bifunctional molecules,<sup>17–19</sup> and to molecules of biological relevance.<sup>20</sup> Besides its sensitivity, this method has the advantage over direct infrared absorption of being isomer selective: the UV wavelength chosen as a probe is set at a transition which corresponds to a given species and enables one to record the vibrational spectrum of selected isomers.

We present here the vibrational spectrum of hydrogen-bonded complexes formed between two different asymmetric molecules. The complexes studied here consist of 2-naphthyl-1-ethanol, denoted NapOH hereafter, and alaninol (2-amino-1-propanol), the alcohol derived from alanine, denoted A hereafter, as a complexing agent. Besides being chiral, alaninol possesses two sites of complexation, the oxygen and nitrogen atoms, which can compete as a hydrogen bond accepting site from NapOH.

\* Corresponding author. E-mail: anne.zehnacker@ppm.u-psud.fr.

Recent IR results<sup>21</sup> have shown that alaninol, like other amino alcohol molecules, exists under several conformers under gas-phase conditions, the most stable of which possesses an internal hydrogen bond. As a result, the only H-bond-accepting site in this stable structure is the oxygen atom. However, the internal H-bond is disrupted in the bulk where intermolecular H-bonds are predominant, and both nitrogen and oxygen can act as H-bond acceptors. This molecule provides therefore an opportunity to study the interplay of inter- and intramolecular H-bonding and the implication of this competition in chiral recognition.

### Experimental Section

The setup used for fluorescence excitation experiments rests on the laser-induced-fluorescence detection of van der Waals complexes formed in a continuous supersonic expansion of helium (2–3 atm). The molecules are excited in the cold region of the jet by means of a frequency-doubled dye laser (DCM) pumped by the second harmonic of a YAG laser (BM Industrie). The fluorescence is observed at right angle through a WG335 cutoff filter by a Hamamatsu R2059 photomultiplier. The signal is monitored by a Lecroy 9400 oscilloscope connected to a PC.

The setup used for the IR/UV double resonance experiments combines a pulsed jet (General Valve) and two 20 Hz OPO lasers (BBO for the visible one and LiNbO<sub>3</sub> for the infrared one). The OPO system consists of an original prototype first developed at the Centre Laser Infrarouge d'Orsay (CLIO) and rests on two OPOs synchronously pumped by a pulsed mode-locked Nd:YAG laser, as described elsewhere.<sup>18</sup> The YAG oscillator is fitted with an intracavity nonlinear absorber in order to generate trains (macropulses) of 50 micropulses at a repetition rate of 20 Hz. The micropulse duration and separation are 12 ps and 10 ns, respectively. The idler beam of the LiNbO<sub>3</sub>/OPO is tunable from 2.6 to 4  $\mu\text{m}$  and has a bandwidth of 3  $\text{cm}^{-1}$  (fwhm) at 3  $\mu\text{m}$ . Its power at 3  $\mu\text{m}$  is 25 mW. The signal beam of the visible has a bandwidth of 3  $\text{cm}^{-1}$  at 550 nm. Its power is maintained at 9 mW.

The IR spectra are recorded with the fluorescence dip IR spectroscopy technique, a variante of the double resonance technique first introduced by Lee<sup>22</sup> and co-workers and pioneered by Tanabe et al.,<sup>23</sup> Riehn et al.,<sup>24</sup> and Pribble et al.<sup>25</sup> Briefly, the fluorescence signal arising from a transition excited by the UV laser is used to monitor the population of the ground-state level of a given complex, and the IR laser frequency is scanned in the region of interest. When  $\nu_{\text{IR}}$  is resonant with an infrared transition from the ground-state species selected by the probe, the IR-induced depletion manifests itself by a dip in the fluorescence intensity. The fluorescence signal used to monitor the IR absorption is averaged over the whole macropulse.

Both 2-naphthyl-1-ethanol and 2-amino-1-propanol under their pure enantiomeric forms have been purchased from Aldrich and used as provided. The chromophore has been used under its *S* form and will be denoted as a capital letter (*S*) in what follows, while the enantiomers of alaninol will be denoted as a lower case letter (*r* or *s*): the homochiral and heterochiral complexes will therefore be called *Ss* and *Sr*, respectively.

### Theoretical Section

The calculation strategy has been already described elsewhere.<sup>18</sup> It is divided into two parts. First, an exploration of a model potential energy surface is performed by means of a semiempirical method in which the intramolecular coordinates are kept frozen. This method has been developed by Claverie<sup>26</sup> and extended by Brenner et al.<sup>27</sup> The model potential energy

**TABLE 1: Calculated Binding Energy by the Claverie Method and by DFT/B3LYP Method, Including BSSE, and with or without ZPE<sup>a</sup>**

complex			$D_c$		$D_0$
			Claverie	B3LYP + BSSE	B3LYP + ZPE + BSSE
NapG1A1a	<i>Ss</i>	cycle	8.1	6.1	4.3
NapG1A1b	<i>Ss</i>	chain	7.9	5.6	4.3
NapG1A2	<i>Ss</i>	bridge	11.6	8.0	6.5
NapG2A1a	<i>Ss</i>	cycle	8.1	7.2	5.6
<i>NapG2A1b</i>	<i>Ss</i>	<i>chain</i>	7.8	5.9	4.5
<i>NapG2A2</i>	<i>Ss</i>	<i>bridge</i>	11.4	8.0	6.8
NapG1A1a	<i>Sr</i>	cycle	7.9	6.6	4.9
NapG1A1b	<i>Sr</i>	chain	8.0	5.9	4.7
NapG1A2	<i>Sr</i>	bridge	11.6	7.9	6.5
NapG2A1a	<i>Sr</i>	cycle	8.1	6.9	5.9
<i>NapG2A1b</i>	<i>Sr</i>	<i>chain</i>	7.8	5.8	4.6
<i>NapG2A2</i>	<i>Sr</i>	<i>bridge</i>	11.4	8.1	6.7

<sup>a</sup> The calculated values in italics are assigned to the experimentally observed complexes.

surface is constructed within the frame of the second order exchange perturbation theory. The interaction energy is given as a sum of four terms: electrostatic, short-range repulsion, polarization, and dispersion.<sup>8,27</sup> Each of these terms is analytically written as a function of the intermolecular distances. An exploration of the potential energy surface is then performed by means of simulated annealing combined with a local optimization of each minimum.<sup>28,29</sup>

As this method only optimizes the energy with respect to the intermolecular degrees of freedom, the second part of the calculation strategy is the full optimization of the most stable complexes obtained previously by means of ab initio calculations. The size of the molecules under investigation precludes the use of correlated methods such as MP2, and we have therefore chosen to use density functional theory (DFT). As will be seen below, the complexes studied here involve “conventional” hydrogen bonds (OH $\cdots$ O or OH $\cdots$ N), which are mainly electrostatic in nature, together with OH $\cdots$  $\pi$  interactions. Tsuzuki and co-workers<sup>30</sup> have discussed the nature of the attractive forces in complexes involving a OH $\cdots$  $\pi$  or NH $\cdots$  $\pi$  interaction and have concluded that electrostatic energy is the main attractive component and is responsible for the directionality of the  $\pi$  H-bond. The use of a method which includes dispersion is therefore not absolutely necessary, and DFT methods seem pertinent for the systems studied here. However, since they do not include dispersion interactions, the absolute value of the binding energy should be taken cautiously.

The calculations have been performed by using the hybrid Hartree–Fock functional density B3LYP with the standard 6-31G\*\* basis set of Gaussian 98.<sup>31</sup> The basis set superposition error (BSSE) has also been calculated by means of the counterpoise method of Boys and Bernardi<sup>32</sup> to obtain the binding energy. Finally, harmonic frequencies calculations have been done for the most stable isomers, and zero-point energy (ZPE) has been included in the binding energy (see Table 1).

### Structure of the Bare Molecules

**NapOH Chromophore.** The structure of the NapOH molecule will be described in another paper.<sup>33</sup> Two isoenergetic conformers of NapOH have been calculated and assigned to the 0–0 transitions located at 31 738 and 31 814  $\text{cm}^{-1}$  (31 738 +76  $\text{cm}^{-1}$ ), respectively. They are very similar: both show a gauche orientation of the hydroxyl group to the C<sub>2</sub>–C <sub>$\alpha$</sub>  bond as well as to the CO bond but they differ by a rotation of the

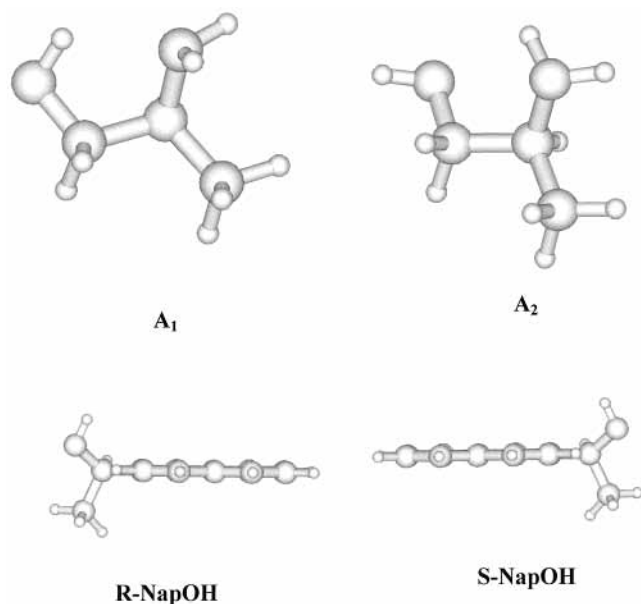


**Figure 1.** Stable conformers of alaninol with an OH $\cdots$ N (denoted as A1) and an NH $\cdots$ O (denoted as A2) intramolecular hydrogen bond, together with the *R* and *S* enantiomers of 2-naphthyl-1-ethanol. These structures were optimized at the B3LYP/6-31G\*\* level. A2 lies 2.5 kcal/mol higher in energy than A1.

aromatic plane of 180° around the C<sub>2</sub>–C<sub>α</sub> axis. They exhibit the same spectrum in the OH stretch region: the  $\nu(\text{OH})$  stretch appears at 3647 cm<sup>-1</sup> and is followed by a weaker band at 3680 cm<sup>-1</sup> assigned to a combination band. They differ by the frequency of the  $\nu(\text{C}^*\text{H})$  stretch localized on the asymmetric carbon atom. The isomers responsible for the bands located at 31 738 and 31 738 cm<sup>-1</sup> + 76 cm<sup>-1</sup> respectively in the excitation spectrum will be called hereafter NapG1 and NapG2.

**Alaninol.** Amino alcohols present several conformations in isolated conditions which have been recently studied and classified by Fausto et al.<sup>21</sup> This classification uses three letters referring respectively to the configurations obtained by rotation around the C–N (g for gauche or rotation of +60°, g' for gauche or rotation of -60°, t for trans or rotation of 180°), the C–C (G, G', or T) and the C–O (g, g', or t) bonds, respectively. The vibrational analysis of their infrared spectrum in the gas phase and in rare gas matrixes<sup>21</sup> led to the conclusion that the most abundant species has a g'Gg' geometry. It has a gauche conformation around the C–C central bond and involves an intramolecular H bond between the OH group as a donor and the amino group as an acceptor. This g'Gg' form shows a red shift of the OH stretch relative to 1-propanol (experimental values of 3579 vs 3676 cm<sup>-1</sup>), due to the OH $\cdots$ N interaction. The  $\nu(\text{NH}_2)_a$  asymmetric stretching motion, though much weaker than the  $\nu(\text{OH})$  stretching mode, is observed at 3405 cm<sup>-1</sup> in the gas phase. The results of our calculations are completely in line with those of Fausto et al. The most stable form, denoted as A1 hereafter, is the same as the g'Gg' form proposed by Fausto and is shown in Figure 1. The O $\cdots$ N distance is 2.74 Å, while the  $\tau(\text{OCCN})$  dihedral angle is 52°, slightly shifted down from the 60° value corresponding to a gauche form by the intramolecular H-bond. The methyl group is in anti position relative to the hydroxy group.

In rare gas matrixes, the presence of a conformer with no OH $\cdots$ N interaction manifests itself by the appearance of a  $\nu(\text{OH})$  band located much to the blue of that of the main form, at 3674 cm<sup>-1</sup>. It has been assigned by Fausto et al. to a less stable (gGt) conformer which possesses a free OH group. We

**TABLE 2: Calculated  $\nu(\text{OH})$  and Asymmetric  $\nu(\text{NH}_2)$  Stretch Frequencies, along with the Experimentally Observed Values<sup>a</sup>**

molecule or complex	$\nu(\text{OH})$ (NapOH)	$\nu(\text{OH})$ (alaninol)	$\nu(\text{NH}_2)_a$	$\nu(\text{NH}_2)_s$
NapOH	3805			
A1		3685 (71)	3576 (0)	3481 (0)
A2		3837 (20)	3574 (4)	3488 (1)
Calculated Ss Complexes				
NapG2A1 (cycle)	3278 (958)	3591 (772)	3556 (8)	3469 (7)
NapG2A1 (chain)	3584* (213)	3548* (441)	3586 (13)	3486 (6)
NapG2A2 (bridge)	3362 (909)	3778 (262)	3569 (5)	3485 (4)
Calculated Sr Complexes				
NapG2A1 (cycle)	3254 (984)	3599 (814)	3556 (1)	3471 (0)
NapG2A1 (chain)	3589* (333)	3550* (361)	3595 (11)	3495 (3)
NapG2A2 (bridge)	3370 (948)	3820 (119)	3570 (5)	3484 (5)
Experimentally Observed Frequencies				
Ss(-94 cm <sup>-1</sup> )	3277	3638	3427	
Ss(-28 cm <sup>-1</sup> )	3440	3405		
Sr(-60 cm <sup>-1</sup> )	3455	3440		

<sup>a</sup> No scaling factor has been applied. The modes denoted by asterisks (\*) are delocalized on both OH groups. The calculated values in italics are assigned to the experimentally observed complexes.

have calculated an A2 form similar to gGt (see Figure 1), which lies 2.5 kcal/mol higher in energy than A1 (B3LYP calculations with the 6-31G\*\* basis set, including ZPE corrections). This conformer is characterized by an intramolecular distance  $d_{\text{O}\cdots\text{N}}$  of 2.81 Å and a dihedral angle  $\tau(\text{OCCN})$  of 63°. As in A1, the methyl group is in anti position relative to the hydroxy group.

The form with an intramolecular OH $\cdots$ N interaction dominates in the gas phase or in rare gas matrixes. The conformational preference of alaninol can, however, be modified by the surroundings, for example in solution, when the involvement of alaninol in hydrogen bonds to a protic solvent results in a competition between intra- and intermolecular OH $\cdots$ N interactions. Though the open structure A2 exists to a minor extent in matrixes, it is dominant in neat alaninol. In the pure liquid, the intermolecular OH $\cdots$ N interactions dominates and the monomeric units preferentially adopt an open type structure (gGt). The frequencies experimentally observed at 3348, 3282, and 3174 cm<sup>-1</sup> have been assigned to the  $\nu(\text{NH}_2)_a$ ,  $\nu(\text{NH}_2)_s$ , and  $\nu(\text{OH})$  stretching modes of hydrogen-bonded alaninol.

In the absence of jet-cooled data, we will use the calculated harmonic frequencies of the g'Gg' and gGt forms. The values of the  $\nu(\text{OH})$  and  $\nu(\text{NH}_2)_a$  stretches frequencies are listed in Table 2. A point worth mentioning is that the  $\nu(\text{NH}_2)_a$  stretch appears as a very strong band in the neat alaninol spectrum, although its calculated intensity is only slightly larger in A2 (4 km/mol) than it is in A1 (almost 0). It is therefore likely that the  $\nu(\text{NH}_2)_a$  asymmetric stretch intensity is enhanced by the involvement of alaninol in intermolecular H-bonded structures.

## Experimental Results

**Laser-Induced Fluorescence.** The laser-induced-fluorescence spectra of the NapOH/A complexes are shown in Figure 2. Besides the bands assigned to the bare molecule whose origin appears at 31 738 cm<sup>-1</sup> and is followed by two bands located at 39 and 76 cm<sup>-1</sup> further to the blue,<sup>2</sup> new intense bands show up at lower energy than the origin. The use of pure enantiomers enables us to assign the bands located at -28 and -94 cm<sup>-1</sup> to the homochiral Ss complex, and that located at -59 cm<sup>-1</sup> to the Sr complex. The intensity dependence of these three bands upon alaninol concentration is linear; they have therefore been assigned to 1:1 complexes. Besides these main bands, much

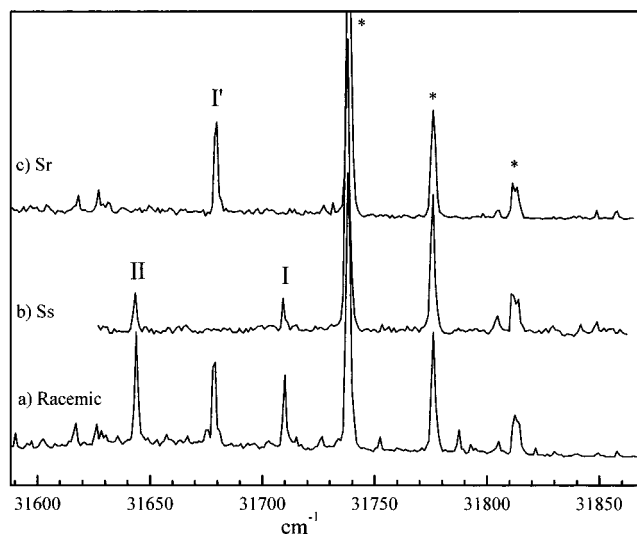


**Figure 2.** Fluorescence excitation spectrum of the NapOH:2-amino-1-propanol complexes. (a) Racemic mixture. (b) Ss complex. (c) Sr complex. The bands due to the bare chromophore are denoted by asterisks (\*). The origin transition of the bare chromophore is located at 31 738  $\text{cm}^{-1}$ . The Ss and Sr complexes have been probed on bands I and II, and I', respectively.

weaker (intensity less than 10%) bands due to the Sr diastereoisomer appear further to the red at  $-111.5$  and  $-121$   $\text{cm}^{-1}$  (see Figure 2a,c) and must be due to a complex of minor concentration or larger clusters. The intensity of the observed bands should be corrected by the fluorescence quantum yield to draw a quantitative conclusion about the relative abundance of the corresponding complexes. However, the excited states corresponding to the excitation of these three intense features have the same lifetime of  $(110 \pm 20)$  ns, which shows that their fluorescence quantum yields should be of the same order.

As will be shown below, the two intense bands observed in the Ss complex excitation spectrum are due to two different isomeric forms. They will be denoted band I (excitation at  $-28$   $\text{cm}^{-1}$ ) and band II (excitation at  $-94$   $\text{cm}^{-1}$ ), respectively. In contrast, one fluorescent form of the Sr complex (band I') is observed in our experimental conditions.

The Sr and the two forms of the Ss complexes possess different transition energies, which clearly shows that chiral discrimination is observed in the laser-induced-fluorescence spectrum. This behavior is due to the different structures and binding energy of the diastereoisomeric pairs both in the ground state and in the excited state.

**Infrared Spectroscopy.** The fluorescence dip spectra of the complexes are shown in Figure 3. A rigorous interpretation of the experimental results requires *ab initio* calculations of the most stable structures of the complexes and of their associated harmonic frequencies, which will be presented in the following section. Before doing so we will present the data observed in the OH stretch region and qualitatively analyze them in the light of earlier works: the  $\nu(\text{OH})$  bands observed in the complexes show up in different regions. First, OH groups involved in a strong  $\text{OH}\cdots\text{N}$  hydrogen bond should exhibit a tremendously large red shift and appear below  $3300$   $\text{cm}^{-1}$ . Second, OH groups involved in a weak  $\text{OH}\cdots\text{N}$  or in a  $\text{OH}\cdots\text{O}$  hydrogen bond should appear in the  $3400$ – $3500$   $\text{cm}^{-1}$  range. Last, a  $\pi$ -bonded OH stretch should be slightly shifted down in frequency and appear in the  $3590$ – $3630$   $\text{cm}^{-1}$  range,<sup>34</sup> while the frequency of a free  $\nu(\text{OH})$  should be seen at higher energy and be almost not modified relative to the bare molecule. These four kinds of OH stretch will be denoted by “strong  $\text{OH}\cdots\text{N}$ ”, “intermediate

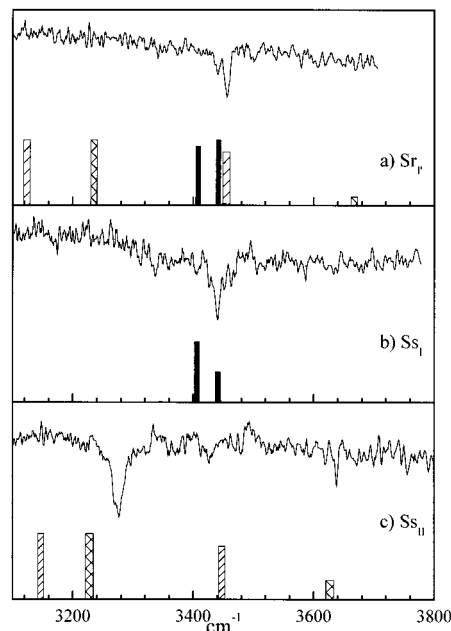


**Figure 3.** Fluorescence dip infrared spectrum of the 1-amino-2-propanol complexes, along with the calculated spectrum. The harmonic frequencies have been scaled by 0.96. The calculated spectrum of the chain complex shown by a bold black line, that of the cyclic complex is shown by ///, and that of the bridged complex by  $\Delta\Delta\Delta$ .

OH” (i.e.,  $\text{OH}\cdots\text{O}$  between two alcohol molecules or weak  $\text{OH}\cdots\text{N}$ ), “ $\text{OH}\cdots\pi$ ”, and “free OH”, hereafter. This approach will enable us to extract qualitative information on the nature of the predominant H-bond interaction between NapOH and alaninol.

**Sr Complex (UV Probe on Band I').** The fluorescence dip spectrum recorded with the probe set on the transition located at  $-59$   $\text{cm}^{-1}$  from the origin of the bare molecule is shown in Figure 3a. As expected for a complex with two hydroxy groups, two bands appear in the OH stretch region as an intense doublet located at  $3455$ – $3441$   $\text{cm}^{-1}$ . Besides being much more intense than the  $\nu(\text{OH})$  band of the bare molecule, both components of the doublet show a larger breadth (about  $6$   $\text{cm}^{-1}$ ) and are red shifted by  $192$  and  $206$   $\text{cm}^{-1}$ , respectively, relative to bare NapOH. This shift indicates a hydrogen bond of intermediate strength (for example, the  $\nu(\text{OH})$  frequency is  $3501$   $\text{cm}^{-1}$  in the NapOH– $\text{CH}_3\text{OH}$  complex and around  $3420$   $\text{cm}^{-1}$  in the NapOH– $(\text{CH}_3\text{OH})_2$  complex<sup>33</sup>). It is to be noted that no band appears above  $3600$   $\text{cm}^{-1}$ , which is an indication that neither the chromophore nor the solvent contains a free OH group. Also, no band with a very large red shift is observed, which indicates that no strong  $\text{OH}\cdots\text{N}$  interaction is present in the complex. One of these two bands must therefore be due to  $\nu(\text{OH})$  of NapOH acting as a donor in a  $\text{OH}\cdots\text{O}$  bond to the solvent, and the other one is due to the OH stretch of alaninol involved in the intramolecular H-bond. Both observed bands are red shifted relative to the  $\nu(\text{OH})$  frequency of both NapOH and the A1 and A2 conformers of alaninol. We can qualitatively deduce from these experimental results that the structure of the Sr complex involves an  $\text{OH}\cdots\text{O}$  intermolecular bond.

**Ss Complex (UV Probe on Band I).** The fluorescence dip spectrum recorded with the probe set on the transition located at  $-28$   $\text{cm}^{-1}$  from the origin of the bare molecule is shown in Figure 3b. At first sight, it bears strong similarity with the fluorescence dip spectrum of the Sr complex described above. Despite a less satisfying signal-to-noise ratio than that observed in the Sr spectrum, due to the weaker fluorescence signal, a similar pattern is observed in the  $\nu(\text{OH})$  region for both

species: here again, no band appears in the region of the free OH stretch, and a doublet is observed more to the red, which led us to the conclusion that the structure is probably similar to that of the Sr complex described above. However, a closer look at the spectrum enables one to see some subtle differences: the most intense component of the doublet appears at  $3440\text{ cm}^{-1}$  while a much weaker band appears more to the blue at  $3464\text{ cm}^{-1}$ .

**Ss Complex (Band II).** The IR spectrum recorded with the probe set on the band located at  $-94\text{ cm}^{-1}$  of the origin (Figure 3c) shows a completely different pattern, with a dramatic difference in the  $\nu(\text{OH})$  region. A very broad ( $20\text{ cm}^{-1}$ ) and intense band appears at  $3276\text{ cm}^{-1}$ . The huge red shift relative to  $\nu(\text{OH})$  of bare NapOH is typical of a strong H-bond such as an  $\text{OH}\cdots\text{N}$  interaction. A similar red-shifted  $\nu(\text{OH})$  band is observed in the case of the hydrated complex of 2-amino-1-phenylethanol ( $3349\text{ cm}^{-1}$ ).<sup>19</sup> Moreover, a sharp band of medium intensity appears at  $3638\text{ cm}^{-1}$ , in the energy range where the frequency of the OH groups involved in an  $\text{OH}\cdots\pi$  interaction are expected to appear (for example, the  $\nu(\text{OH})$  frequency is  $3639\text{ cm}^{-1}$  in benzene- $\text{CH}_3\text{OH}$ <sup>34</sup>). Last, a very weak band appears at  $3427\text{ cm}^{-1}$ , attributable to a  $\nu(\text{NH})$  stretch. The structure of this complex therefore completely differs from that described above: the internal H-bond of the solvent is absent. Instead, a strong hydrogen bond between the OH group of NapOH and the  $\text{NH}_2$  group of the solvent and a weak  $\text{OH}\cdots\pi$  interaction between the OH group of the solvent and the aromatic ring take place.

### Theoretical Results

As mentioned before, the first step of our calculation strategy is a whole exploration of the potential energy surface with the internal geometry of the components kept frozen. It is therefore important to use physically relevant conformations of the subunits as starting geometries for this calculation. The experimental results described above indicate that, in one of the observed Ss complexes, the alaninol fragment possesses an intramolecular hydrogen bond, while it is absent in the other one. We have therefore chosen as starting geometry the most stable of the alaninol conformers with an intramolecular H bond (A1) and the most stable of the conformers with no hydrogen bond (A2). Though the energy difference between A1 and A2 is large (2.5 kcal/mol), the conformer of alaninol involved in the aggregation process in solution is the open structure A2.<sup>21</sup> It should participate in the aggregation processes in the gas phase as well.

Calculations have been performed with both A1 and A2 together with both NapG1 and NapG2 as starting points for the energy optimization. The binding energy has then been calculated relative to that of the subunits as starting points: for example, the energy of a complex built from NapG2 and A1 as a starting point will be calculated relative to that of bare NapG2 and A1, and includes the deformation energy. The binding energies of the most stable structures calculated with different methods (Claverie, B3LYP corrected for BSSE and with or without ZPE) are given in Table 1.

The number of calculated structures is much higher than that observed experimentally. It seems however that the complexes with only one of the conformers of NapOH are observed experimentally. Owing to the similarity between NapG1 and NapG2, the complexes built on the two conformers have very similar structures and frequencies. As the complexes built on NapG2 are slightly more stable than that built on NapG1, and their calculated spectra match the experimentally observed data

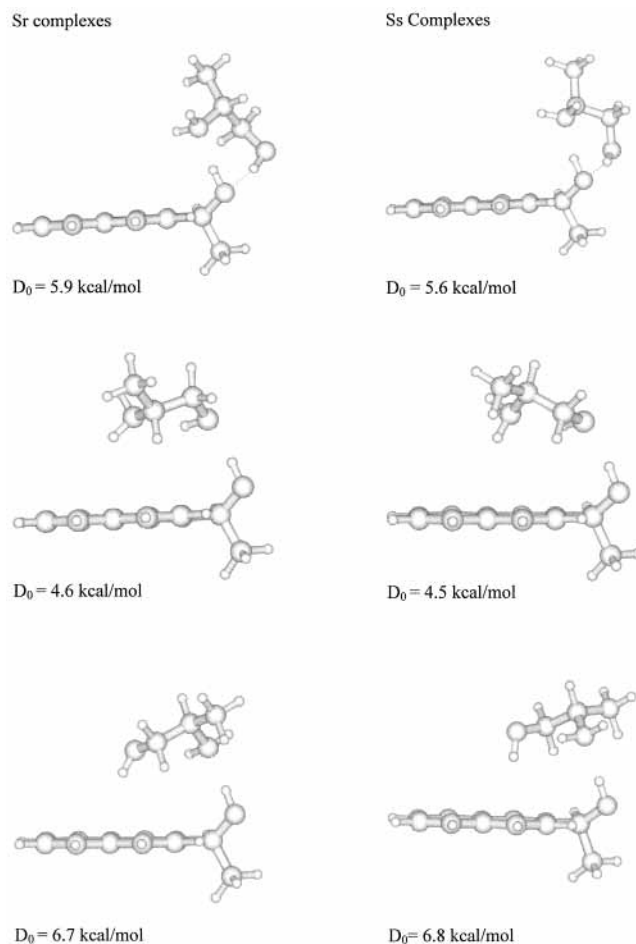


**Figure 4.** Calculated most stable geometry of the Sr and Ss complexes, respectively. (top) Cyclic complex (built from A1). (middle) Chainlike complex (built from A1). (bottom) Bridged complex (built from A2).

a little better, we will assume hereafter that the experimentally observed complexes are those formed between NapG2 and alaninol. The structures of the most stable complexes with NapG2 are given in Figure 4. The structural parameters related to the intermolecular distances and angles, together with the intramolecular dihedral angle  $\tau(\text{OCCN})$ , which characterizes the structure of alaninol, are given in Table 3 for the complexes considered hereafter.

**Sr Complex.** The optimization of structures built on the A1 conformer of alaninol and the NapG2 conformer of NapOH leads to complexes which can be classified in two families: The most stable complex (binding energy of 5.9 kcal/mol) corresponds to a “cyclic” complex: the hydroxyl group of the chromophore is inserted within the intramolecular bond of the A1 conformer of alaninol. This results in a structure exhibiting two strong intermolecular interactions: an  $\text{OH}\cdots\text{N}$  interaction between the OH group of the chromophore and the nitrogen atom of alaninol ( $d_{\text{O}\cdots\text{N}} = 2.77\text{ \AA}$ ), and an  $\text{OH}\cdots\text{O}$  interaction between the hydroxyl group of alaninol and the oxygen atom of NapOH ( $d_{\text{O}\cdots\text{O}} = 2.83\text{ \AA}$ ). The intramolecular  $\text{OH}\cdots\text{N}$  distance is longer ( $3.04\text{ \AA}$ ) than in the bare molecule and the dihedral angle  $\tau(\text{OCCN})$  opens up from  $52^\circ$  in bare A1 to  $70^\circ$  in the complex: in other words, the intramolecular bond loosens up to allow the insertion of the hydroxyl group of NapOH.

The second family of complexes will be called hereafter the “chain” family. The calculated binding energy of the most stable complex of this family is 4.6 kcal/mol. In this complex, the intramolecular bond of alaninol is maintained, and even reinforced ( $d_{\text{O}\cdots\text{N}} = 2.67\text{ \AA}$ ), while the main interaction between

**TABLE 3: Structural Characteristics of the Calculated Molecules and Complexes<sup>a</sup>**

molecule or complex	dihedral angle $\tau(\text{OCCN})$ (deg)	intramolecular distance $d_{\text{O}\cdots\text{N}}$ (Å)	$\alpha(\text{OH}\cdots\text{N})$ angle (deg)	intermolecular distance $d_{\text{O}\cdots\text{O}}$ (Å)	$\alpha(\text{OH}\cdots\text{N})$ angle (deg)	intermolecular distance $d_{\text{O}\cdots\text{N}}$ (Å)	$\alpha(\text{OH}\cdots\text{N})$ angle (deg)
A1 <i>S</i> (R) enantiomer	52 (−52)	2.74	118				
A2 <i>S</i> (R) enantiomer	63 (−63)	2.81					
			Ss Complex				
NapG2A1 cycle	70	3.04		2.81	159	2.79	165
NapG2A1 chain	46	2.67	123	2.83	171		
NapG2A2 bridge	55	2.80				2.85	176
			Sr Complex				
NapG2A1 cycle	−73	3.07		2.83	166	2.77	165
NapG2A1 chain	−47	2.67	123	2.83	174		
NapG2A2 bridge	−57	2.77				2.86	174

<sup>a</sup> The calculated values in italics are assigned to the experimentally observed complexes.

NapOH and alaninol is an  $\text{OH}\cdots\text{O}$  intermolecular bond between the hydroxyl group of the chromophore and the oxygen atom of alaninol ( $d_{\text{O}\cdots\text{O}} = 2.83$  Å) as shown Figure 4. We can note that the intramolecular bond of alaninol is shortened because complexation with NapOH enhances the acidity of the OH group of alaninol.

A third family of complexes, the “bridge” family, is obtained when optimizing the structure build on the A2 conformer of alaninol. The calculated binding energy is much higher (6.7 kcal/mol) than that of the complexes of the “cyclic” and “chain” types. This complex exhibits two kinds of intermolecular interactions: a strong  $\text{OH}\cdots\text{N}$  bond between the hydroxyl group of NapOH and the nitrogen atom of alaninol ( $d_{\text{O}\cdots\text{N}} = 2.86$  Å), and a much weaker one between the hydroxyl group of alaninol and the  $\pi$  system of the chromophore. In this case the rearrangement of alaninol induced by complexation is the modification of the dihedral angle  $\tau(\text{HOCC})$ , which is  $-166^\circ$  in the isolated molecule and  $-107^\circ$  in the complex. This modification corresponds to a rotation of the OH group toward the aromatic ring which allows the  $\text{OH}\cdots\pi$  interaction to take place.

The calculated  $\nu(\text{OH})$  and  $\nu(\text{NH}_2)_a$  frequencies are given in Table 2 for the bare molecules and the three types of complexes. The calculated spectra are also shown Figure 3 with the frequencies corrected by the frequently used scaling factor of 0.96 for a better comparison with the experimental data. The calculated spectra of the cyclic, chainlike, and bridged complex clearly differ from each other: the spectrum of the chainlike complex exhibits a doublet in the  $3400\text{ cm}^{-1}$  region, showing that the two hydrogen bonds are of similar strength. On the other hand, both the cyclic and bridged complexes show a  $\text{OH}\cdots\text{N}$  interaction, which manifests itself by the appearance in both spectra of a strong band shifted much further to the red, in the  $3200\text{ cm}^{-1}$  region. This band is obviously not observed in the experimental spectrum. It seems therefore reasonable to assign the experimentally observed Sr complex to the chainlike species. The  $\nu(\text{NH}_2)$  asymmetric stretch of alaninol is calculated to appear in the same energy range as the  $\nu(\text{OH})$  stretches, and its calculated oscillator strength is much lower than that of  $\nu(\text{OH})$  (10 vs 357 or 308 km/mol). Despite its calculated intensity being 2 orders of magnitude smaller than that of  $\nu(\text{OH})$ , a  $\nu(\text{NH}_2)$  asymmetric stretch has been observed in the ion dip spectrum of 2-amino-1-phenylethanol, which exhibits a similar intramolecular hydrogen bond.<sup>19</sup> As pointed out by the authors, the depletion intensity of a given transition depends not only on the oscillator strength of the transition but also on the depletion efficiency for the vibrationally excited state which is related to IVR and predissociation efficiency. It makes it therefore possible to observe in the same spectrum transitions with very different oscillator strengths. However,

even if present, the weak band due to the  $\nu(\text{NH}_2)$  asymmetric stretch of alaninol must be hidden by the much stronger features due to  $\nu(\text{OH})$ , which precludes its observation.

The direct consequence of the assignment stated above is that the most stable calculated forms of the heterochiral complex (“cycle” or “bridge”) are not experimentally observed, a point to which we shall return in the discussion. It is worth mentioning that the frequency of the  $\nu(\text{OH})$  stretch of alaninol is shifted down in the chainlike complex from its value in the bare molecule, in line with the calculated shorter intramolecular hydrogen bond. This shows that the intramolecular hydrogen bond is reinforced in the complex because the acidity of the hydroxyl group of alaninol is enhanced by its role as a proton acceptor from NapOH. These cooperative effects are well documented in the case of water or methanol dimers bridging the H-donor and H-acceptor parts of bifunctional compounds such as *o*-cyanophenol or pyridone,<sup>17,18</sup> in which the intradimer distance is shortened relative to the isolated species. However, they are more seldom observed for intramolecular H bonds.

**Ss Complexes.** The calculated structures and harmonic frequencies of the Ss complexes parallel those obtained for the Sr complexes. The calculated structures range in three families: the “cycle”, the “chain”, and the “bridge” families. The structures are shown Figure 4, and the associated harmonic frequencies are given in Table 2. The calculated binding energy of the most stable “cycle” complex is 5.6 kcal/mol, and the intermolecular distances  $d_{\text{O}\cdots\text{N}}$  and  $d_{\text{O}\cdots\text{O}}$  are respectively 2.79 and 2.81 Å. The binding energy of the most stable “chain” structure is 4.5 kcal/mol. The intramolecular distance  $\text{O}\cdots\text{N}$  is 2.67 Å (shorter than in isolated alaninol), and the intermolecular  $\text{O}\cdots\text{O}$  distance is 2.83 Å. Last, the most stable complex of the bridge families possesses a binding energy of 6.8 kcal/mol and the geometric parameter is  $d_{\text{O}\cdots\text{N}} = 2.85$  Å for the strong intermolecular bond. As observed in the Sr complex, a weak  $\text{OH}\cdots\pi$  interaction is present. The rearrangement of alaninol induced by complexation manifests itself by the modification of the HOCC angle, which is  $166^\circ$  in the isolated molecule and  $146^\circ$  in the complex.

The calculated frequencies are given in Table 2. The calculated spectra, scaled by 0.96, are shown Figure 3b,c along with the experimental ones. On the basis of the same arguments as put forward for the Sr complexes, we propose to assign the “chain” structure to the isomer that presents an electronic transition red shifted by  $28\text{ cm}^{-1}$  (band I).

The calculated spectrum of the “bridge” structure is characterized by a strong band due to the OH group of NapOH in interaction with the N atom of alaninol, along with a weaker one due to the OH group of alaninol acting as a donor to the aromatic ring. It satisfyingly reproduces the experimental spectrum obtained when the UV probe is set on the transition

located at  $-94\text{ cm}^{-1}$  from the strong NapOH origin (band II). Moreover, a very weak but real band appears at  $3427\text{ cm}^{-1}$  in the experimental spectrum, at exactly the same frequency as that calculated for the  $\nu(\text{NH}_2)$  asymmetric stretch of alaninol in the bridged complex ( $3570\text{ cm}^{-1}$ , i.e.,  $3427\text{ cm}^{-1}$  including the scaling factor). For all these reasons, this isomer has been assigned to a “bridge” structure.

None of the experimental spectra matches that calculated for the cyclic complex. The cyclic Ss complex does not seem to be observed, nor was the cyclic Sr complex, under our experimental conditions.

## Discussion

The fluorescence excitation and fluorescence dip spectra clearly show that two major isomers of the homochiral complex are stabilized in the supersonic expansion, while only one fluorescent form of the heterochiral pair is observed. Aided by the DFT calculations, it has proved possible to assign one of the homochiral pairs as well as the solely observed heterochiral complex to a “chain” complex. In this complex, the NapOH chromophore is anchored to alaninol through a  $\text{OH}\cdots\text{O}$  bond. The structure of alaninol within this “chain” complex is only slightly modified relative to its most stable structure in isolated conditions, and the intramolecular H-bond is preserved. In the other experimentally observed homochiral complex, the main interaction is an intermolecular  $\text{OH}\cdots\text{N}$  interaction between the NapOH hydroxy group and the amino group of alaninol. This interaction overcomes the intramolecular H-bond which is therefore disrupted in the complex.

These results invite two comments: First, the most stable calculated complex (“cycle”) is never observed. Second, the “bridge” complex is only observed for the homochiral pair.

It is first to be noted that the bridged Ss complex is built from (*S*)-NapOH and the A2 conformer of (*S*)-alaninol. Its binding energy is 6.8 kcal/mol, but the total energy of the A2 conformer is 2.5 kcal/mol higher than that of the A1 conformer. Taking this difference into account, the total energy of the Ss bridged complex with NapOH and A1 as dissociation limits ( $-4.3\text{ kcal/mol}$ ) is higher than that of the most stable Ss cyclic complex ( $-5.6\text{ kcal/mol}$ ). The same considerations hold for the Sr complexes: the total energy of the Sr bridged complex ( $-4.2\text{ kcal/mol}$ ) with NapOH and A1 as dissociation limits is higher than that of the most stable Sr cyclic complex ( $-5.9\text{ kcal/mol}$ ). One can deduce from this energetic considerations that the most stable calculated complex, for both the Sr and Ss diastereoisomers, is the “cyclic” complex. In this structure, the intramolecular hydrogen bond of alaninol is disrupted to allow the insertion of the OH group of naphthylethanol between the amino group and the hydroxyl group of alaninol. None of the fluorescence dip spectra experimentally observed matches that calculated for the cyclic complex. It seems therefore reasonable to take for certain that this complex is not formed under our experimental conditions or not detected by LIF.

At first sight, it is surprising that the most stable calculated complex is not formed. A first explanation for this unexpected behavior can be obtained from the comparison between the reorganization energies calculated for the different complexes under study. By “reorganization energy”, we mean the difference between the energy of the molecular components within the complex and that of their most stable conformation as isolated fragments. The reorganization energy involves mainly the deformation of the alaninol moiety and is about 0.5 kcal/mol in the bridged or chainlike complexes, while it amounts to almost 3 kcal/mol in the cyclic complex. As the formation of

1:1 complexes in the collision zone of the expansion requires three-body collisions, it is likely that the bare molecules are at least partially cooled prior to complex formation. The complexes would therefore be formed in a second step with no extensive structural reorganization of their components. With this in mind, it is conceivable that the formation of complexes requiring a large reorganization of the fragments is accompanied by a high energy barrier and is therefore disfavored. In other words, the complex formation is kinetically rather than thermodynamically controlled: only the complexes whose formation does not require overcoming a large energy barrier are observed, even if they are not the most stable.

The fact that cyclic complexes are not observed seems to be a general trend in NapOH complexes<sup>33</sup> and those of its benzenic analogue 1-phenylethanol (PetOH)<sup>35</sup> or benzyl alcohol.<sup>36,37</sup> The structure of the 1:2 complexes of PetOH or NapOH with water or methanol consists of a solvent dimer linking the hydroxy group and the aromatic ring. This contrasts with phenol, whose dihydrated complex exhibits a ring structure.<sup>12</sup> The phenol OH group is also able to insert in the hydrogen-bonded bridge of a carboxylic acid dimer.<sup>38</sup> These different behaviors can be explained by considering the acid–base properties of the chromophore: NapOH is a weaker acid than phenol and competes less efficiently with the intramolecular hydrogen bond. It is a weaker base as well, and as a result the aromatic ring can efficiently compete with the hydroxyl group to accept a hydrogen bond.

It is worth comparing the present systems with another complex involving an amino alcohol molecule, 2-amino-1-phenylethanol: in its singly hydrated complex,<sup>19</sup> the intramolecular H-bond is disrupted by the first bound water molecule. This results in the formation of the analogue of the “cyclic” complex, which is not experimentally observed in our case. The difference between these two systems can be explained by the difference in size between NapOH and water, which can insert much more easily for steric reasons.

The second point we have to discuss is the lack of experimental observation of the “bridge” Sr complex, while the “bridge” Ss complex is responsible for the most intense transition in the excitation spectrum. However, one has to keep in mind that our detection rests on laser-induced fluorescence and, as pointed out previously,<sup>3</sup> the fluorescence lifetime of the NapOH complexes varies in a nonregular way with the excess energy and the size of the cluster. The apparent elusiveness of the “bridge” Sr complex could be explained by its low fluorescence quantum yield. To support this hypothesis, we can mention the existence of bands of much lower intensity in the excitation spectrum of the Sr complex, located at  $-115.5$  and  $-121\text{ cm}^{-1}$ . Owing to their weak intensity, these bands have not been probed, and we cannot rule out the hypothesis that these bands are due to the bridge form of the Sr complex.

## Conclusion

Fluorescence dip spectroscopy has been applied to the diastereoisomeric complexes of (±)-2-naphthyl-1-ethanol with (±)-2-amino-1-propanol. Aided by DFT calculations, it has been possible to characterize the structure of the different complexes under investigation. The Ss and Sr complexes differ by the number of observed isomers: while both oxygen and nitrogen atoms of alaninol can act as an hydrogen bond accepting site for the OH group of the chromophore in the Ss pair, leading to the formation of both “chain” and “bridge” complexes, only one fluorescent form of the Sr complex has been observed. The most stable calculated complex, which corresponds to the

insertion of the chromophore within the intramolecular bond of alaninol, has not been observed experimentally. A possible explanation for this behavior is that the complex formation is under kinetic control: despite being thermodynamically favored, the formation of the cyclic complex requires a wide modification of the fragment's structure relative to the bare species. This process is accompanied by a large energy barrier and is therefore kinetically disfavored. The observation of both "chain" and "bridge" complexes allows us to conclude that complexes containing alaninol either in its most stable geometry in the gas phase (A1) or in solution (A2) coexist under the conditions of a supersonic expansion. Further studies on other bifunctional compounds are currently in progress, the aim of which is to characterize the influence of strength of the intramolecular H-bond on the geometry of the complex.

## References and Notes

- (1) Filippi, A.; Giardini, A.; Piccirillo, S.; Speranza, M. *Int. J. Mass Spectrom.* **2000**, *198*, 137.
- (2) Al-Rabaa, A.; Br  h  ret, E.; Lahmani, F.; Zehnacker, A. *Chem. Phys. Lett.* **1995**, *237*, 480.
- (3) Al Rabaa, A.; Le Barbu, K.; Lahmani, F.; Zehnacker-Rentien, A. *J. Phys. Chem. A* **1997**, *101*, 3273.
- (4) Al Rabaa, A.; Le Barbu, K.; Lahmani, F.; Zehnacker-Rentien, A. *J. Photochem. Photobiol., A* **1997**, *105*, 277.
- (5) Latini, A.; Satta, M.; Giardini-Guidoni, A.; Piccirillo, S.; Speranza, M. *Chem. Eur. J.* **2000**, *6*, 2.
- (6) Mons, M.; Piu  zzi, F.; Dimicoli, I.; Zehnacker, A.; Lahmani, F. *Phys. Chem. Chem. Phys.* **2000**, *2*, 5065.
- (7) Lahmani, F.; le Barbu, K.; Zehnacker-Rentien, A. *J. Phys. Chem. A* **1999**, *103*, 1991.
- (8) Le Barbu, K.; Brenner, V.; Milli  , P.; Lahmani, F.; Zehnacker-Rentien, A. *J. Phys. Chem. A* **1998**, *102*, 128.
- (9) Le Barbu, K.; Lahmani, F.; Zehnacker-Rentien, A. A spectroscopic Study Discrimination in Jet-cooled van der Waals Complexes: The Role of Conformational Isomerism as Studied by Double Resonance Spectroscopy. In *Physical Chemistry of Chirality*; Hicks, J., Ed.; Elsevier: New York, 2001.
- (10) Bohro, N.; Haeber, T.; Suhm, M. A. *Phys. Chem. Chem. Phys.* **2001**, *3*, 1945.
- (11) King, A. K.; Howard, B. J. *Chem. Phys. Lett.* **2001**, *348*, 343.
- (12) Ebata, T.; Fujii, A.; Mikami, N. *Int. Rev. Phys. Chem.* **1998**, *17*, 331.
- (13) Brutschy, B. *Chem. Rev.* **2000**, *100*, 3891.
- (14) Gruenloh, C. J.; Carney, J. R.; Hagemester, F. C.; Arrington, C. A.; Zwier, T. S.; Fredericks, S. Y.; Wood, J. T., III; Jordan, K. *J. Chem. Phys.* **1998**, *109*, 6601.
- (15) Gruenloh, C. J.; Florio, G. M.; Carney, J. R.; Hagemester, F. C.; Zwier, T. S. *J. Phys. Chem. A* **1999**, *103*, 496.
- (16) Gruenloh, C. J.; Hagemester, F. C.; Carney, J. R.; Zwier, T. S. *J. Phys. Chem. A* **1999**, *103*, 503.
- (17) Florio, G. M.; Gruenloh, C. J.; Quimpo, R. C.; Zwier, T. S. *J. Chem. Phys.* **2000**, *113*, 11143.
- (18) Broquier, M.; Lahmani, F.; Zehnacker-Rentien, A.; Brenner, V.; Milli  , P.; Peremans, A. *J. Phys. Chem. A* **2001**, *105*, 6841.
- (19) Graham, R. J.; Kroemer, R. T.; Mons, M.; Robertson, E. G.; Snoek, L. C.; Simons, J. P. *J. Phys. Chem. A* **1999**, *103*, 9706.
- (20) Robertson, E. G.; Simons, J. P. *Phys. Chem. Chem. Phys.* **2001**, *3*, 1.
- (21) Fausto, R.; Cacela, C.; Duarte, M. L. *J. Mol. Struct.* **2000**, *550*, 365.
- (22) Page, R. H.; Shen, Y. R.; Lee, Y. T. *J. Chem. Phys.* **1988**, *88*, 4621.
- (23) Tanabe, S.; Ebata, T.; Fujii, M.; Mikami, N. *Chem. Phys. Lett.* **1993**, *215*, 347.
- (24) Riehn, C.; Lahmann, C.; Wassermann, C.; B., B. *Ber. Bunsen-Ges. Phys. Chem.* **1992**, *96*, 1161.
- (25) Pribble, R. N.; Zwier, T. S. *Science* **1994**, *265*, 75.
- (26) Claverie, P. *Intermolecular Interactions from diatomics to biopolymers*; Pullman, B., Ed.; Wiley: New York, 1978.
- (27) Brenner, V.; Milli  , P. *Z. Phys. D.* **1994**, *30*, 327.
- (28) Metropolis, N.; Rosenbluth, A.; Teller, A.; Teller, E. *J. Chem. Phys.* **1953**, *21*, 1087.
- (29) Bockish, F.; Liotard, D.; Rayez, J. C. *Int. J. Quantum Chem.* **1992**, *44*, 619.
- (30) Tsuzuki, S.; Honda, K.; Uchimaru, T.; Mikami, M.; Tanabe, K. *J. Am. Chem. Soc.* **2000**, *122*, 11450.
- (31) Frisch, M. J.; Trucks, G. W.; Schlegel, H. B.; Scuseria, G. E.; Robb, M. A.; Cheeseman, J. R.; Zakrzewski, W. G.; Montgomery, J. J. A.; Stratmann, E.; Burant, J. C.; Dapprich, S.; Millam, J. M.; Daniels, A. D.; Kudin, K. N.; Strain, M. C.; Farkas, O.; Tomasi, J.; Barone, V.; Cossi, M.; Cammi, R.; Mennucci, B.; Pomelli, C.; Adamo, C.; Clifford, S.; Ochterski, J.; Petersson, G. A.; Ayala, P. Y.; Cui, Q.; Morokuma, K.; Malick, D. K.; Rabuck, A. D.; Raghavachari, K.; Foresman, J. B.; Cioslowski, J.; Ortiz, J. V.; Baboul, A. G.; Stefanov, B. B.; Liu, G.; Liashenko, A.; Piskorz, P.; Komaromi, I.; Gomperts, R.; Martin, R. L.; Fox, D. J.; Keith, T.; Al-Laham, M. A.; Peng, C. Y.; Nanayakkara, A.; Challacombe, M.; Gill, P. M. W.; Johnson, B.; Chen, W.; Wong, M. W.; Andres, J. L.; Gonzalez, C.; Head-Gordon, M.; Replogle, E. S.; Pople, J. A. *Gaussian 98*, Revision A.7; Gaussian, Inc.: Pittsburgh, PA, 1998.
- (32) Boys, S.; Bernardi, F. *Mol. Phys. B* **1970**, *19*, 553.
- (33) Le Barbu, K.; Lahmani, F.; Zehnacker-Rentien, A. Submitted for publication in *J. Phys. Chem. A*.
- (34) Pribble, R. N.; Hagemester, F.; Zwier, T. S. *J. Chem. Phys.* **1997**, *106*, 2145.
- (35) Broquier, M.; Le Barbu, K.; Lahmani, F.; Mons, M.; Zehnacker, A. *Phys. Chem. Chem. Phys.* **2001**, *3*, 4684.
- (36) Guchait, N.; Ebata, T.; Mikami, N. *J. Chem. Phys.* **1999**, *111*, 8438.
- (37) Mons, M.; Robertson, E. G.; Simons, J. P. *J. Phys. Chem. A* **2000**, *104*, 1430.
- (38) Imhof, P.; Roth, W.; Janzen, C.; Spangenberg, D.; Kleinermanns, K. *Chem. Phys. Lett.* **1998**, *242*, 141. (a) Sr complex (probe set on band I' at  $-59\text{ cm}^{-1}$ ). (b) Ss complex (probe set on band I at  $-28\text{ cm}^{-1}$ ). (c) Ss complex (probe set on band II at  $-94\text{ cm}^{-1}$ ).